Induction of pancreatic neoplasia in the *KRAS*/*TP53* Oncopig: preliminary report

Neesha S. Patel[1,2], Katie Bailey[1,2], Audrey J. Lazenby[3], Mark A. Carlson[1,2,4]

1. Department of Surgery, University of Nebraska Medical Center, Omaha, Nebraska
2. Department of Surgery and VA Research Service, Nebraska-Western Iowa Health Care System, Omaha, NE
3. Department of Pathology, University of Nebraska Medical Center, Omaha, Nebraska
4. Department of Genetics, Cell Biology and Anatomy, University of Nebraska Medical Center, Omaha, Nebraska

Running title: Pancreatic neoplasia in the Oncopig

Financial Support: this work was funded by grants from the University of Nebraska Medical Center, the Buffett Cancer Center, and the National Cancer Institute.

Correspondence:
Mark A. Carlson
Surgery 112, VA Medical Center
4101 Woolworth Ave
Omaha, NE 68105 USA
001-402-650-4219
macarlso@unmc.edu

ABSTRACT

Introduction. Five-year survival (all patients) from pancreatic cancer (PC) is in the range of 10%, and has not changed substantially in decades. Current murine models may not adequately mimic human PC, and can be inadequate for device development, which all may contribute to the lack of progress in PC survival. We attempted PC induction in transgenic swine (expressing *KRAS* and *TP53* mutants) with the ultimate goal of creating a more accurate model of PC.

Methods. Transgenic Oncopigs (n = 16, malensrrc.missouri.edu; somatic LSL cassette with $TP53^{R167H}$ and $KRAS^{G12D}$) were injected via laparotomy with AdCre (10^{10} vp/mL) ± IL-8 (0.5-2 ng; a tumor induction adjunct facilitating adenoviral entry into epithelia and promoting local inflammation) into the main pancreatic duct (MPD; via duodenotomy) or duct to the isolated pancreatic connecting lobe (CL). Subjects were necropsied after ≤10 wk, followed by histology.

Results. A total of 16 OCM subjects underwent an induction procedure. Of these, 14 received pancreatic AdCre injection, and nine of these (64%) developed pancreatic tumor (10 if the very first subject which died prematurely is counted). All of these subjects expired within 2-4 weeks after the tumor induction procedure. All had a similar terminal course: failure to thrive, which was secondary to gastric outlet obstruction, which was secondary to a peripancreatic phlegmon, which was secondary to pancreatitis, which appeared to be secondary to tumor. One additional OCM (no. 1088) had a small amount of extrapancreatic tumor at necropsy when it was euthanized for pneumonia at day 113. None of the OCM subjects that underwent a control

injection procedure (no AdCre) nor any of the WT littermates that underwent AdCre injection with or without IL-8 developed pancreatitis.

Conclusion. This proof of principle study demonstrated that PC can be induced in the Oncopig, which has inducible expression of activated KRAS and inactive p53 under control of a floxed stop codon. However, induced subjects will need to live longer to yield a useable PC model. Addition of IL-8 may have contributed to the severe pancreatitis and early mortality. Future studies will focus on modulation of pancreatitis and optimization of the survival period.

INTRODUCTION

Pancreatic cancer (PC) is the 14th most common cancer and the 7th highest cause of cancer mortality in the world.[1] Globally, the number of deaths, incident cases, and disability-adjusted life-years had doubled from 1990 to 2017.[2] Patients with Stage I PC (tumor is less than 2.0 cm with no involved lymph nodes)[3] have a 39% 5-year survival while patients with Stage IV PC (tumor of any size with distant metastases) have an 11% 5-year survival.[4] Surgical resection is the only chance for a cure, but only 15-20% of patients have resectable disease.[3] Despite the development of multimodal therapy, long-term survival is achieved for only 5% of patients.[5]

Due to ethical and practical concerns regarding human experimentation, animal models have become essential in cancer research;[6] murine models in particular have been used in the preclinical study of pancreatic cancer,[7-10] including xenografted immunodeficient models, genetically engineered mouse (GEM) models, humanized mice, and *in vivo* edited mice.[10-19] While murine modeling has produced tremendous advances in the understanding and treatment of cancer in general, the fact remains that only a few percent of drug candidates identified in preclinical studies as potential anti-cancer treatments will be demonstrated to be safe and efficacious in clinical trials, with subsequent FDA approval.[8,18,20,21] Murine models frequently have less-than-ideal accuracy in predicting human biology and response to interventions, secondary to differences in genomic sequence and phenotype; this inaccuracy may contribute to the above inefficiency of the drug pipeline for cancer therapeutics.[10-12,14,15]

Currently there are no large animal models for PC. Swine have shown to be effective models in other fields, including in trauma, transplantation, cardiovascular disease, and dermatologic conditions.[22,23] Swine have greater similarity to humans with respect to size,

anatomy, physiology, pathophysiological responses, and genetic sequence than do mice.[24,25] It therefore is conceivable that swine could have greater accuracy in cancer modeling than mice currently do. Importantly, the human-relevant size of certain porcine breeds allows for research and development of devices, imaging techniques, interventional technologies, and so forth, which would be difficult if not infeasible in a twenty-gram mouse.

Concurrent with the sequencing of the porcine genome and the increased availability and tractability of genetic editing technologies, work has ensued on porcine cancer modeling, including for breast, liver, colorectal, and pancreatic tumors.[26-30] In 2015 a transgenic swine known as the Oncopig Model (OCM) was described,[31] which utilized a Cre-Lox system to control expression of a somatic cassette containing porcine *KRAS*^{G12D} and *TP53*^{R167H}. The expressed KRAS mutant was constitutively activated, while the p53 mutant functioned as a dominant negative. The OCM is the porcine analogue of the KPC mouse.[32] Previously we attempted induction of PC in the OCM with introduction of relatively low doses of adenovirus expressing Cre recombinase (AdCre) into the OCM pancreatic duct, but we did not obtain tumor.[33] Herein we report more aggressive attempts to induce PC in the OCM, with resultant tumor generation.

METHODS AND MATERIALS

Standards, Rigor, Reproducibility, and Transparency

To the extent possible, the animal studies of this report were designed, performed, and reported in accordance with both the ARRIVE recommendations[34] (Animal Research: Reporting of *In Vivo* Experiments) and the National Institutes of Health Principles and Guidelines for Reporting Preclinical Research;[35] for details and exceptions, refer to Supplemental Information.

Animal Welfare Statement

The animals utilized to generate the data for this report were maintained and treated in accordance with the *Guide for the Care and Use of Laboratory Animals* (8th ed.)[36] and also in accordance with the Animal Welfare Act of the United States (U.S. Code 7, Sections 2131 – 2159). The animal protocol pertaining to this manuscript was approved by the Institutional Animal Care and Use Committee (IACUC) of the VA Nebraska-Western Iowa Health Care System (ID number 1124) and by the IACUC of the University of Nebraska Medical Center (ID number 19-053-FC). All procedures were performed in animal facilities approved by the Association for Assessment and Accreditation of Laboratory Animal Care International (AAALAC; www.aaalac.org) and by the Office of Laboratory Animal Welfare of the Public Health Service (grants.nih.gov/grants/olaw/olaw.htm). All surgical procedures were performed under isoflurane anesthesia, and all efforts were made to minimize suffering. Euthanasia was performed in accordance with the AVMA Guidelines.[37]

Experimental Subjects

Transgenic Oncopigs (Oncopig Model, or OCM) and their wild type (WT) littermates were purchased from the National Swine Research and Resource Center (NSRRC) at the University of Missouri Columbia (nsrrc.missouri.edu). The OCM subjects were a hybrid of Minnesota minipigs and domestic pigs. Genotype of each porcine subject was confirmed with PCR upon subject delivery (Supplemental Information). Swine were housed two littermates per pen, except for one week of individual housing post-laparotomy (but still with contact through the pen grating), in order to prevent wound cannibalism. Swine were fed ad lib with standard hog feed (Purina Nature's Match® Sow and Pig Complete Feed; www.purinamills.com).

Reagents

Ad5CMVCre-eGFP (AdCre) was purchased from University of Iowa Vector Core (vector-core.medicine.uiowa.edu). Porcine IL-8 was purchased from Novus Biological (NBP2-35234; novusbio.com). General chemicals were purchased from Millipore Sigma (www.sigmaaldrich.com).

Experimental Design.

The basic experimental design included a ≥1 week acclimatization period after subject delivery to the research facility. PCR confirmation of genotype was performed during this

period. Each subject then would undergo an induction procedure (laparotomy under general anesthesia; one major survival procedure), followed by an observation for up to 3 mo.

Survival Procedure: Set-Up and Anesthesia

Swine were fasted for 24 h prior to the procedure, with free access to water. On day zero, subjects were weighted, and underwent induction with ketamine (2.2 mg/kg), Telazol® (1:1 w/w tiletamine:zolazepam, 4.4 mg/kg) and xylazine (2.2 mg/kg), given as a single IM injection. EKG, pulse oximetry, and lingual end-tidal CO_2 monitors were placed and connected to a BM5 Bionet monitor (bionetus.com). Endotracheal intubation was performed with a 6-7 mm ID tube. The subject rested on a water-circulated warming blanket that was set at 102˚F. An auricular intravenous (IV) line was placed, and LR was administered at 500mL/hr. Cefovecin sodium (Convenia®; 8 mg/kg IM) and Buprenorphine SR (0.2mg/kg SC) were administered during the induction period. Anesthesia was maintained with isoflurane (1-2%) and supplemental oxygen (3-5 L/min) using Matrx® ventilator (midmark.com). The ventilator rate initially was set at 12-15 breaths per minute with a tidal volume of 8 mL/kg, and subsequently adjusted to maintain the EtCO2 at 40-50 mm Hg. Phlebotomy was performed on a forelimb or auricular vein. The ventral abdomen, groins, and thorax were scrubbed with chlorhexidine soap, and then the ventral abdomen was depilated with electric clippers. Cotton blankets were placed over non-surgical areas to minimize subject heat loss. The final abdominal preparation was performed with alcohol-based chlorhexidine (ChloraPrep™; bd.com), and then the upper midline region was sterilely draped.

Survival Procedure: Tumor Induction

Laparotomy and Exposure. A 12 cm upper midline laparotomy incision was made. Abdominal wall retraction was maintained with a self-retaining abdominal (Bookwalter) retractor. The long tongue of the spleen was placed into the right upper quadrant. The small intestine was held inferiorly with laparotomy pads and the self-retaining retractor. The pylorus was identified, grasped, and brought up to the incision. The proximal pancreas could be elevated with the pylorus and proximal duodenum; this maneuver provided access to both the anterior and posterior surface of the proximal pancreas (see Results and Discussion). The colon typically was lightly adherent to the anterior surface of the pancreas with loose connective tissue, so the colon was mobilized inferiorly with scissors.

Injection of Tumor Induction Reagent. There were three basic techniques of injecting the tumor induction reagent into the pancreas: (1) injection into the main pancreatic duct with parenchymal injections; (2) injection into the duct of the connecting lobe of the pancreas; and (3) technique 2 plus parenchymal injections. The induction reagent consisted of AdCre (adenovirus expressing Cre recombinase) at a concentration of $1x10^{10}$ PFU/100 µL (in saline), with an injection volume of 200 µL. Some subjects (see Results and Discussion) also received porcine IL-8 (5 ng/mL; 200 µL volume) mixed in with the AdCre, and given as one injection.

Technique 1: Main Duct + Parenchyma. After the above exposure of the pancreas had been obtained, a 3-cm longitudinal enterotomy was made on the anti-mesenteric side of the duodenum, directly opposite to the termination of the duodenal lobe of the pancreas into the duodenal wall, which was the location of the papilla of the main pancreatic duct (MPD). The incised duodenal walls were retracted laterally with silk stay sutures. The MPD then was directly cannulated with a 20-gauge plastic catheter (Angiocath™ IV

Catheter; Becton Dickinson) and injected with the induction reagent (Fig. S1A). Parenchymal injections were also performed in some subjects on the anterior and posterior side of the proximal duodenal lobe of the pancreas (typically two injections on each side, using a 25-gauge needle). Each parenchymal injection site was marked with small dot (1-2 mm wide) of India ink, using a 27-gauge needle. The duodenal enterotomy then was closed in two layers, using a running 3-0 polyglactin 910 suture for the inner row, full-thickness, inverting (Connell) technique. This was followed with an outer seromuscular row of interrupted 3-0 silk sutures (Lembert technique).

Technique 2: Connecting Lobe. After exposure of the pancreas was obtained, the connecting lobe of the pancreas was identified where it joined the proximal duodenal lobe (see Results & Discussion). The connecting lobe then was doubly clamped and transected about 1 cm inferior to the junction with the duodenal lobe. The proximal stump of the connecting lobe (against the duodenal lobe) was tied off with a 3-0 silk ligature. Using operative loupe (3.5x) magnification, the open end of the primary duct running through the connecting lobe was found in the free cut end of that lobe (see Results and Discussion). This duct was cannulated with a 20-gauge plastic catheter, and the induction reagent was injected into the duct of the connecting lobe. The catheter was withdrawn, and the free end of the connecting lobe then was immediately ligated with 3-0 silk.

Laparotomy Closure. The abdominal incision was closed anatomically in layers, with running 3-0 polyglactin 910 in the peritoneum and posterior sheath, running 0-polydioxanone in the anterior aponeurosis, 3-0 polyglactin 910 in the panniculus carnosus, and 4-0 polyglactin 910 in the dermis. Cyanoacrylate glue was applied over the skin incision; no other incisional dressing

was applied. The animal's recovery from anesthesia was monitored until the subject was awake and mobile. Subjects were given half feeds on post-induction day 1, and were placed back on ad lib feeds by day 2.

Study Termination and Euthanasia

The prescribed post-induction observation period was three months. Criteria for early removal from the study and euthanasia were symptoms of failure to thrive (anorexia, lethargy, decreased movement, abnormal breathing, or other signs of distress) or sepsis (fever, wound disruption or drainage). At time of euthanasia, each subject received sedation with ketamine/Telazol/xylazine, as described above, and then endotracheally intubated. Inhalational isoflurane (5%) was administered via the ventilator. The prior midline incision was reopened. Inferiorly this incision was extended in paramedian fashion to avoid midline structures such as the urethra in males. The necropsy incision extended from xiphoid to the pelvic inlet. The bilateral thoracic cavity was entered by transversely incising the diaphragm just inferior to the xiphoid. The intrathoracic portion of the inferior vena cava was easily identified as it emerged from the liver in the posterior mediastinum. Phlebotomy was performed from the cava, and then Fatal-Plus® (pentobarbital sodium, 390 mg/mL; 1 mL per 4.5 kg body weight) was administered by caval injection. Two minutes after administration of Fatal-Plus®, the inferior vena cava was transected just above the diaphragm to exsanguinate the subject. A gross necropsy involving the lungs, heart, liver, kidneys, pancreas, intestines, bladder, and associated peritoneal surfaces then was performed, with biopsy of any suspicious lesions.

Tissue processing, Histology and Immunohistochemistry

Tissue was either formalin fixed and sent for further processing, or fresh tissue was taken and digested for *in vitro* analysis. Tissue that was cut from formalin-fixed samples was stained with H&E for pathological examination. IHC was performed by deparaffinizing slides and heating using citric acid antigen retrieval buffer (Vector laboratories, H3300). Following antigen retrieval, endogenous peroxidases were quenched with 3% hydrogen peroxide solution for 5 min. Blocking was done using 2.5% horse serum blocking buffer (Vectastain Elite ABC HRP ready-to-use kit) for 30 min prior to primary antibody application. Antibodies included anti-mutant p53 (abcam, ab32049), anti-RAS^{G12D} (Vita Scientific, NEBA10124), and anti-Pan-Keratin. Primary antibodies were incubated overnight at 4°C. Staining then was developed using HRP-conjugated secondary antibody followed by DAB substrate (DAKO).

Immunoblotting

Tissue from the tumor was cultured and protein extraction was performed with lysis buffer (Pierce protease and phosphatase inhibitor mini tablet, A32961 and Pierce RIPA buffer, 89901) with needle homogenization. Protein quantification was performed with a BCA assay. Samples were mixed with sample buffer and an equal amount of protein (20-30 µg) were boiled for 5 min, separating on a 10-15% SDS-PAGE gel and transferred to a nitrocellulose membrane. The membrane was blocked using Odyssey blocking buffer (927-40000; Licor.com) for 1 h and incubated with the primary antibodies against at 4°C overnight. The membrane then was washed three times (5 min per wash) with TBS-T. Fluorescent secondary antibody was incubated for 1 h

followed by 3 more washes. Protein bands were visualized using the BIO-RAD imager for fluorescent detection. All immunoblots were performed in triplicate.

Cell Culture

Tumor tissue was washed in PBS, and minced into cubic millimeter pieces with a razor blade. The minced tissue was put in 1 mg/mL collagenase I solution with 100 ug/mL of DNase I, and placed into the incubator at 10 min intervals followed by activate digestion with a 10 mL pipette for 45 min. The digested tissue was then filtered using 100 µm filter, spun down at 300 *g* at 4˚C for 5 min. The supernatant was removed, and the cell pellet was washed with Epithelial Cell Media (ECM; Sigma) with 5% FBS, followed by an additional 5 min spin. Cells were layered into a 6-well plate coated with porcine gelatin for 1 h to allow adhesion of cellular debris and non-epithelial cells to the plate. The media containing epithelial cells was then transferred to a fresh 6-well coated plate, and cells were allowed to adhere overnight at 37˚C. The next day cells were washed with PBS and allowed to grow until 80% confluency before splitting into a 10-cm coated dish.

RESULTS & DISCUSSION

Cadaveric Anatomical Dissection

The tri-lobar structure of the pancreas has previously been described.[38] In anticipation of performing tumor induction procedures on the porcine pancreas, we performed some gross dissections of the pancreas and surrounding structures in fresh porcine carcasses, immediately after euthanasia. These subjects (domestic swine, 50-60 kg) already had been scheduled for euthanasia on an unrelated research protocol, in which no intraabdominal procedures had been done. Our rationale to perform these procedures was to achieve a greater understanding of gross anatomy of the porcine pancreas (which is somewhat different from the gross anatomy of the human pancreas), and to optimize performance of our induction procedures.

In humans, the pancreas is mostly retroperitoneal in location; the anterior surface of the pancreatic head and body is covered with peritoneum. In contrast, the proximal half porcine pancreas is mostly peritonealized, which allows the proximal organ to be lifted upwards without any surgical dissection. This unique anatomic characteristic of the porcine pancreas facilitates and speeds most surgical procedures on that organ, as operations on the human pancreas typically require extensive dissection to expose the organ. In the pig, simply grasping the pylorus and proximal duodenum and lifting anteriorly brings the pancreas into the surgical incision, and provides adequate surgical exposure to both the anterior and posterior surface of the proximal pancreas. In essence, the C-loop of the duodenum (which wraps around the proximal pancreas n both humans and pigs) functions as a floppy mesentery in the pig.

In humans, the pancreas has been given somewhat arbitrary anatomical boundaries of "head" (adjacent to the duodenum and to the right of the portomesenteric vein), "neck" (overlying the portomesenteric vein), "body" (to the left of the portomesenteric vein), "tail" (near the splenic hilum), and a variably present uncinate process which comes off the inferior side of the pancreatic head.[39] In the pig, however, there are three fairly distinct lobes which interconnect to form the pancreas: the duodenal, splenic, and connecting lobes (Fig 1-3). These lobes form a continuous ring, which affords a unique opportunity for surgical intervention and tumor induction, as detailed below.

The duodenal lobe of the porcine pancreas (Fig. 1A-B) is an elongate structure situated inferiorly to the pylorus and gastric antrum. The proximal end of the duodenal lobe tapers to a termination on the mesenteric border of duodenal C-loop, 10-15 cm distal to the pylorus. At this point the main pancreatic duct traverses the duodenal wall and opens into the duodenal lumen via the pancreatic papilla. There is no pancreatic head per se in the porcine pancreas (an no uncinate process). In humans, the pancreatic head is a more globular structure which gives the pancreas recognizable girth where it abuts the duodenum. In the pig, the "head" region of the pancreas is the smoothly tapered end of the duodenal lobe. Another difference between pigs and humans is the duodenal entry point of the common bile duct. In humans, the common bile duct typically joins with the main pancreatic duct within the head of the pancreas, and the combined ducts enter the duodenum at the Ampulla of Vater. In the pig, the common bile duct and main pancreatic duct do not join; the former enters the duodenum individually via the biliary papilla, which is post-pyloric, 8-10 cm proximal to the pancreatic papilla. It is the duodenal lobe of the porcine pancreas which is mostly visible (anteriorly and posteriorly) when the pylorus and duodenum are elevated into the surgical incision.

The splenic lobe of the porcine pancreas (Fig. 1A-B) is another elongate structure which initiates at the distal end of the duodenal lobe, and terminates near the splenic hilum. The splenic lobe is more of a retroperitoneal structure, and thus less accessible. The exception to this is the distal tip of the splenic lobe (Fig. 1A); this tip is peritonealized, and has a thumb-like appearance as it emerges from the retroperitoneum, just inferior to the hilum of the spleen. Its anatomical configuration and location make it amenable to open surgical biopsy during a survival procedure. We have performed such biopsy in >10 pigs (in separate studies) with no apparent perioperative consequences, and no obvious issues at subsequent necropsy.

The connecting lobe of the porcine pancreas (Fig. 1A-D) is a structure unique to the pig, and has no real equivalent in humans. The connecting lobe is a U-shaped structure which connects the mid-portion of the duodenal lobe to the mid-portion of the splenic lobe. This tri-lobar configuration forms a continuous ring of the porcine pancreas, within which runs a continuous circular ductal system (Fig. 1B). This circular configuration is reminiscent of the arterial Circle of Willis at the base of the human brain. The main pancreatic duct of the pig exits from this circular ductal system within the duodenal lobe (Fig. 1B), and continues proximally to enter the duodenum, as described above. This unique circular anatomy of the porcine pancreas affords a unique surgical opportunity, in that the ring could be safely interrupted for an intervention (e.g., ductal injection, Fig. 1C-D). After such an interruption, the ductal system should be capable of retrograde decompression away from the interruption point, and not be obstructed—if it is assumed that the circular ductal system of the porcine pancreas is indeed a complete circle.

Connecting Lobe Injection in WT Pigs

As mentioned in the Introduction, we had previously attempted tumor induction in the OCM (N = 5), but did not obtain gross tumor after 4 mo observation.[33] For those induction procedures, AdCre (the induction reagent) was injected into the main pancreatic duct and parenchyma of the duodenal lobe (Technique 1 in the Methods) at a dose of 1×10^8 pfu. Some histologic abnormalities were noted (proliferative ductal lesions), but none of these appeared to be cancerous. Of note, Schook et al.[40] observed a diffuse nodular thickening of the main pancreatic duct which histologically appeared to be adenocarcinoma in one OCM subject, 12 mo after intraductal injection of 4×10^9 pfu of AdCre. We hypothesized that if we increased our dose of AdCre that was injected into the pancreatic duct, then we should obtain ductal cancer in the OCM.

One issue that we noted with our previous group of OCM subjects[33] was that after injection of AdCre into main pancreatic duct, the continual flow of pancreatic secretion rapidly flushed the injectate out of the papilla and into the duodenal lumen. This flushing rapidly diluted the AdCre, likely decreasing its efficacy. In order to prevent this flushing, the pancreatic duct would need to be ligated. However, ligation of the main pancreatic duct would obstruct the entire ductal system (Fig. 1A-B), which presumably would have profound and dangerous consequences to the subject. We hypothesized that we could instead transect the isthmus region of the proximal connecting lobe (Fig. 1A-D), cannulate and inject a pancreatic duct in this location, and then immediately ligate the duct ends with impunity. This maneuver would minimize loss of the injectate, which thus would be in contact with the ductal epithelium for a longer duration than had the duct not been ligated.

In order to determine whether interruption of the isthmus portion of the connecting lobe with cannulation of the pancreatic duct within the connecting lobe (Fig. 1A-D) would feasible and well-tolerated, we undertook this procedure in WT domestic pigs (N = 5; 3-4 mo, 30-45 kg), injecting saline distally into the connecting lobe, with ligation of both cut ends of that lobe (i.e., infection technique 2 in the Methods). This effectively interrupted the circular configuration of the porcine pancreas. At operation, the duct within the transected connecting lobe was small (≤1 mm), but could accommodate insertion of a 20-gauge plastic catheter (Fig. 1B), and flushed easily with 1.0 mL of saline. All five pigs tolerated the connecting lobe injection procedure without difficulty. All pigs underwent necropsy one month after operation, and there was no gross evidence of pancreatic inflammation (data not shown).

Induction of Tumor in OCM Subjects: Technique #1

As discussed above, we elected to give a higher dose of AdCre (2×10^{10} pfu) with the current experiments than what we used before (1×10^{8} pfu), which represented more than a 100-fold increase in the dose of AdCre. We also elected to administer IL-8 as an adjunct with the AdCre; this cytokine has been shown to mobilize the adenoviral receptor to the lumenal membrane of epithelial cells, thereby enhancing viral entry.[41,42] We these two conditions we intended to increase our chances for successful pancreatic tumor induction in the OCM.

The first subject in this report (no. 468 in Table 1) underwent induction with technique #1 (i.e., AdCre + IL-8 injection into the main pancreatic duct + injections into the parenchyma of the duodenal lobe); see Fig. 2A. This subject died unexpectedly over a weekend 17 days after the induction procedure. The carcass was refrigerated and the necropsy was performed 72 h later.

The subject had a gastric perforation with extensive peritoneal soilage (Fig. 2B). The cause of the gastric perforation was gastric outlet obstruction, which in turn was caused by a peripancreatic phlegmon (Fig. 2C). Unfortunately, reasonably intact tissue could not be obtained for histology secondary to the prolonged interval between death and necropsy. The second subject underwent a similar tumor induction, and underwent euthanasia/necropsy on day 73 (planned endpoint), with no gross or microscopic evidence of tumor.

We hypothesized that injecting reagents into the main pancreatic duct was not allowing efficient AdCre action secondary to the flushing phenomenon described above. We therefore elected to perform connecting lobe injection (technique #2) in all subsequent tumor inductions. We also decided to forgo the concomitant parenchymal injections, secondary to the concern that a parenchymal injection would expose a wide variety of cell types (pancreatic ductal cells, islet cells, fibroblasts, endothelial cells) to AdCre and possible transformation. Pleomorphic or sarcomatous tumor induction with non-directed AdCre injection in the OCM has been observed by Schook's group.[31,40] We reasoned that injection of AdCre exclusively into a pancreatic duct should keep viral exposure mostly confined to the epithelial cells lining the lumen of the duct, and therefore produce tumor that would be (mostly) an adenocarcinoma.

Induction of Tumor in OCM Subjects: Technique #2

Pancreatic tumor induction with AdCre ± IL8 injection into the connecting lobe (technique #2) was attempted in 12 OCM subjects (Table 2). Only two of these subjects (no. 473 and 475) lived to their planned euthanasia data without incident, and had no remarkable findings at gross necropsy nor with microscopic analysis. However, nine of these subjects (75%) had

onset of lethargy and decreased feeding at 10-15 days after the induction procedure, with progressive decline that necessitated unplanned euthanasia at a mean of 18 ± 7 days (range 10-31). The gross findings at necropsy in these nine subjects was similar to that in OCM no. 468 above (technique #1; unexpected death), that being a peripancreatic phlegmon producing gastric outlet obstruction (Fig. 3A,C; Fig. 4B). In each case the phlegmonous process had obliterated the region in and around the proximal pancreas; in some cases there was gross liquefaction. It was difficult to discern anatomical landmarks around the phlegmon. In addition, six of the subjects with tumor had a varying number of intraabdominal nodules (<1 cm) studding the surface of various structures (Fig. 3A), including the omentum, mesentery, diaphragm, liver, spleen, parietal peritoneum, stomach, and intestines.

The initial concern was that AdCre injection into the connecting lobe of the OCM subjects was inciting a severe pancreatitis that indirectly lead to subject demise from gastric outlet obstruction. However, upon cutting into the phlegmon of these subjects, there was a firm pale core, which appeared to be tumor (Fig. 4A). H&E microscopy of slices taken from the core of the peripancreatic phlegmon from all nine subjects that underwent premature euthanasia demonstrated wide regions of tumor (Fig. 4C-E). Tumor cells had large nuclei with prominent nucleoli. Tumor cell morphology varied from spindle-shaped to rounded. Sheets of tumor cells were interspersed with normal appearing pancreatic acini and the occasional islet, along with areas of liquefaction necrosis and hemorrhage. Areas of tumor were often surrounded by areas of activated lymphocytes (Fig. 4C-D). In addition, there were numerous tumor-infiltrating lymphocytes and macrophages, and occasionally neutrophils and eosinophils. In some subjects there were numerous multi-nucleated giant cells which appeared to be engulfing vacuoles of necrotic material. Preliminary immunohistochemistry of tumor from the peripancreatic phlegmon

suggested that these tumors were of mixed and dedifferentiated phenotype, variably staining with epithelial and mesenchymal markers.

In the subjects that had tumor nodules outside of the phlegmon, these grossly appeared to be “drop” or contact metastases, being only present on the surface of the involved organ or tissue, and mostly inferior and ventral to the phlegmon. There was no evidence of nodule formation contained within the body of an organ, such as the liver. Histologic evaluation of these extra-pancreatic nodules revealed them to be dedifferentiated tumor with a prominent component of activated lymphocytes, both around and within the tumor. In some cases these tumor implants showed evidence of invasion into the underlying normal tissue, with disruption of the peritoneum and underlying connective tissue capsule covering the normal tissue.

The remaining, as yet undescribed subject (no. 1088) in this group of 12 OCM underwent unplanned euthanasia at day 113 secondary to respiratory distress. At necropsy there was gross evidence of acute pneumonia; on histology, the pulmonary alveoli filled with fluid and acute inflammatory cells. There also were several nodules (≤1 cm) on the surface of the anterior stomach, but the pancreas was unremarkable. Histologic evaluation of the gastric nodules demonstrated dedifferentiated tumor, similar to the above extrapancreatic nodules. This subject also had sheets of activated lymphocytes present on H&E sections of the liver, spleen, and lung. This suggested the presence of an additional unknown process, which included the possibility of a hematologic malignancy.

Control Injections in OCM and WT Pigs

Similar injections (technique #2) of tumor-induction agents (AdCre ± IL-8) into the connecting lobe of non-transgenic pigs (N = 6; WT littermates of the OCM subjects; Table 2) were performed in order to determine whether the procedure or the induction agents would induce any pathology in the background breed of the OCM. All WT subjects tolerated the injection without difficulty, and there were no remarkable finding at necropsy. H&E evaluation of the connecting lobe of the pancreas in these subjects revealed minimal chronic inflammation, but otherwise was unremarkable. In order to determine whether some condition unique to the transgenic pig (and not necessarily tumor) was producing severe pancreatitis after the connecting lobe procedure, two OCM subjects underwent IL-8 injection only into the connecting lobe (no. 1101 and 1087 in Table 1). These two subjects tolerated the procedure without difficulty, and had no remarkable findings at necropsy. The results of the control injections from both WT and OCM subjects suggested that the severe inflammatory response noted in AdCre-treated OCM subjects was secondary to tumor formation.

Implications for Future Study

This proof-of-principle study demonstrated that tumor could be induced in the pancreas of the KRAS/p53 Oncopig. However, the time course was fulminant (sometimes <2 wk), and the subjects succumbed to a secondary complication of the tumor (gastric outlet obstruction), not necessarily the tumor itself. The intense inflammatory reaction associated with the tumor may have been secondary to an acute load of neoantigens that flooded these juvenile-aged subjects with an intact and vigorous immune system. Another possible cause of this reaction may have

been a response to adenoviral infection; however, this is unlikely, since none of the WT pigs similarly treated with AdCre developed pancreatitis.

While pancreatic tumor induction is indeed feasible in the Oncopig, the current status of a porcine model of pancreatic cancer is that further development is needed. The time course of tumor development in this study was too rapid for the model to be amenable for research purposes. The clinical course of tumor development might be slowed by decreasing the current dose of AdCre—with the understanding that prior experiments that used lower doses of AdCre produced no tumor at all. Another option might be to use a different viral vector (e.g., lentivirus), which might result in lower levels of AdCre expression.

The associated T-cell inflammatory response, which appeared to be a major underlying cause of rapid subject demise, might be mitigated with administration of immunosuppression. However, use of immunosuppression would increase the model complexity and might impact model relevance. The fields of tumor immunomodulation and tumor immunoediting currently are under intense study,[19,43-45] and tumor interactions with the immune system in these OCM subjects could be highly relevant. Secondary to these realities, and the concerns over clinical relevance of tumor xenografting in immunodeficient mice,[9,46] it was our intent from the outset of these studies to develop a large animal model of pancreatic cancer in immunocompetent subjects.

Another possible issue with tumor induction in the present study was the pleomorphic and sometimes dedifferentiated appearance of the tumor cell populations. It was not clear whether these tumors were mostly epithelial in nature (i.e., resembling pancreatic ductal adenocarcinoma), or something else. Even though the AdCre was injected into the pancreatic duct, it still may have been possible for AdCre infection and transformation of non-epithelial cells. The frequent presence of intraabdominal drop metastases in the OCM subjects suggested

that intraperitoneal spillage of the AdCre during the injection procedure may have occurred, with resultant formation of peritoneally-located tumor nodules. So non-specific transformation may still be an issue, even with the highly-specific connecting lobe injection procedure described in this report. This non-specificity might be addressed in the future with a new transgenic pig, derived from the OCM, in which expression of the transgenes would be restricted to ductal epithelium using a tissue-specific promoter.

Summary

A total of 16 OCM subjects underwent an induction procedure. Of these, 14 received pancreatic AdCre injection, and nine of these (64%) developed pancreatic tumor (10 if the very first subject which died prematurely is counted). All of these subjects expired within 2-4 weeks after the tumor induction procedure. All had a similar terminal course: failure to thrive, which was secondary to gastric outlet obstruction, which was secondary to a peripancreatic phlegmon, which was secondary to pancreatitis, which appeared to be secondary to tumor. One additional OCM (no. 1088) had a small amount of extrapancreatic tumor at necropsy when it was euthanized for pneumonia at day 113. None of the OCM subjects that underwent a control injection procedure (no AdCre) nor any of the WT littermates that underwent AdCre injection with or without IL-8 developed pancreatitis.

ACKNOWLEDGEMENTS

This study is the result of work supported in part with resources and the use of facilities at the Omaha VA Medical Center (Nebraska-Western Iowa Health Care System). Portions of this study were presented at the 50th Annual Joint Meeting of the American Pancreatic Association and Japan Pancreas Society in Maui, Hawaii during November 2019, and at the 15th Annual Academic Surgical Congress in Orlando, FL during February 2020. The authors would like to acknowledge the technical assistance of Chris Hansen. The authors also would like to thank Larry Schook, Tony Hollingsworth, Kyle Schachtschneider, Paul Grippo, Ajay Maker, and Ron Gaba for their helpful comments, insights and suggestions.

Table 1. Tumor induction method and outcome in OCM and WT control pigs.

Serial#	Type	Sex	MPD	CL	AdCre	IL-8	CNI	Day	Euthanasia reason	Gross outcome	Microscopic outcome
468	OCM	M	+	–	+	+	-	17	Died prematurely	PP, GOO	Not available
469	OCM	M	+	–	+	+	-	73	Planned endpoint	Unremarkable	Unremarkable
470	OCM	M	–	+	+	+	-	12	Illness	PP, GOO	Pancreatic tumor
471	OCM	M	–	+	+	+	-	14	Illness	PP, GOO	Pancreatic tumor
472	OCM	M	–	+	+	+	-	14	Illness	PP, GOO	Pancreatic tumor
473	OCM	M	–	+	+	-	-	59	Planned endpoint	Unremarkable	Unremarkable
474	OCM	M	–	+	+	+	-	22	Illness	PP, GOO	Pancreatic tumor
475	OCM	M	–	+	+	+	-	35	Planned endpoint	Unremarkable	Unremarkable
476	WT	M	–	+	-	–	-	35	Planned endpoint	Unremarkable	Unremarkable
477	WT	M	–	+	+	–	-	35	Planned endpoint	Unremarkable	Unremarkable
478	WT	M	–	+	-	–	-	33	Planned endpoint	Unremarkable	Unremarkable
479	WT	M	–	+	+	–	-	36	Planned endpoint	Unremarkable	Unremarkable
481	WT	M	–	+	+	+	-	28	Planned endpoint	Unremarkable	Unremarkable
482	WT	M	–	+	+	+	-	28	Planned endpoint	Unremarkable	Unremarkable
1102	OCM	M	–	+	+	-	-	31	Illness	PP, GOO	Pancreatic tumor
1101	OCM	M	-	+	-	+	-	121	Planned endpoint	Unremarkable	Unremarkable
1088	OCM	M	-	+	+	-	-	113	Illness	Pneumonia	Pneumonia; peritoneal tumor
1087	OCM	F	-	+	-	+	-	121	Planned endpoint	Unremarkable	Unremarkable
1095	OCM	F	-	+	+	+	+	10	Illness	PP, GOO	Pancreatic tumor
1096	OCM	F	-	+	+	-	+	27	Died prematurely	PP, GOO	Pancreatic tumor
1090	OCM	M	-	+	+	+	+	15	Illness	PP, GOO	Pancreatic tumor

1092	OCM	M	-	+	+	-	+	14	Illness	PP, GOO	Pancreatic tumor

IL-8 = interleukin 8; AdCre = adenovirus expressing Cre recombinase; CL = pancreatic connecting lobe injection (technique #2); CNI = cyclosporine, Day = length of survival after induction, in days; GOO = gastric outlet obstruction; MPD = main pancreatic duct injection (technique #1); OCM = Oncopig model; PP = peripancreatic phlegmon; WT = wild type.

References

1. McGuigan A, Kelly P, Turkington RC, Jones C, Coleman HG, McCain RS. Pancreatic cancer: A review of clinical diagnosis, epidemiology, treatment and outcomes. *World J Gastroenterol*. 2018;24(43):4846-4861. PMID: 30487695. DOI: 10.3748/wjg.v24.i43.4846
2. G. B. D. Pancreatic Cancer Collaborators. The global, regional, and national burden of pancreatic cancer and its attributable risk factors in 195 countries and territories, 1990-2017: a systematic analysis for the Global Burden of Disease Study 2017. *Lancet Gastroenterol Hepatol*. 2019;4(12):934-947. PMID: 31648972. DOI: 10.1016/S2468-1253(19)30347-4
3. National Comprehensive Cancer Network. Pancreatic Adenocarcinoma, Version 1.2020. 26 November 2019. In: NCCN Clinical Practice Guidelines In Oncology (NCCN Guidelines®) [Internet]. NCCN. Available from: https://www.nccn.org.
4. Kamarajah SK, Burns WR, Frankel TL, Cho CS, Nathan H. Validation of the American Joint Commission on Cancer (AJCC) 8th Edition Staging System for Patients with Pancreatic Adenocarcinoma: A Surveillance, Epidemiology and End Results (SEER) Analysis. *Ann Surg Oncol*. 2017;24(7):2023-2030. PMID: 28213792. DOI: 10.1245/s10434-017-5810-x
5. van Roessel S, Kasumova GG, Verheij J, Najarian RM, Maggino L, de Pastena M, Malleo G, Marchegiani G, Salvia R, Ng SC, de Geus SW, Lof S, Giovinazzo F, van Dam JL, Kent TS, Busch OR, van Eijck CH, Koerkamp BG, Abu Hilal M, Bassi C, Tseng JF, Besselink MG. International Validation of the Eighth Edition of the American Joint Committee on Cancer (AJCC) TNM Staging System in Patients With Resected Pancreatic Cancer. *JAMA Surg*. 2018;153(12):e183617. PMID: 30285076. DOI: 10.1001/jamasurg.2018.3617
6. Gengenbacher N, Singhal M, Augustin HG. Preclinical mouse solid tumour models: status quo, challenges and perspectives. *Nat Rev Cancer*. 2017;17(12):751-765. PMID: 29077691. DOI: 10.1038/nrc.2017.92
7. Olive KP, Tuveson DA. The use of targeted mouse models for preclinical testing of novel cancer therapeutics. *Clin Cancer Res*. 2006;12(18):5277-5287. PMID: 17000660. DOI: 10.1158/1078-0432.CCR-06-0436
8. Sharpless NE, Depinho RA. The mighty mouse: genetically engineered mouse models in cancer drug development. *Nat Rev Drug Discov*. 2006;5(9):741-754. PMID: 16915232. DOI: 10.1038/nrd2110
9. Siolas D, Hannon GJ. Patient-derived tumor xenografts: transforming clinical samples into mouse models. *Cancer Res*. 2013;73(17):5315-5319. PMID: 23733750. DOI: 10.1158/0008-5472.CAN-13-1069
10. Talmadge JE, Singh RK, Fidler IJ, Raz A. Murine models to evaluate novel and conventional therapeutic strategies for cancer. *Am J Pathol*. 2007;170(3):793-804. PMID: 17322365. DOI: 10.2353/ajpath.2007.060929
11. Begley CG, Ellis LM. Drug development: Raise standards for preclinical cancer research. *Nature*. 2012;483(7391):531-533. PMID: 22460880. DOI: 10.1038/483531a
12. Cook N, Jodrell DI, Tuveson DA. Predictive in vivo animal models and translation to clinical trials. *Drug Discov Today*. 2012;17(5-6):253-260. PMID: 22493784. DOI:
13. Day CP, Merlino G, Van Dyke T. Preclinical mouse cancer models: a maze of opportunities and challenges. *Cell*. 2015;163(1):39-53. PMID: 26406370. DOI: 10.1016/j.cell.2015.08.068

14. Ebos JM, Kerbel RS. Antiangiogenic therapy: impact on invasion, disease progression, and metastasis. *Nat Rev Clin Oncol*. 2011;8(4):210-221. PMID: 21364524. DOI: 10.1038/nrclinonc.2011.21
15. Francia G, Cruz-Munoz W, Man S, Xu P, Kerbel RS. Mouse models of advanced spontaneous metastasis for experimental therapeutics. *Nat Rev Cancer*. 2011;11(2):135-141. PMID: 21258397. DOI: 10.1038/nrc3001
16. Maddalo D, Manchado E, Concepcion CP, Bonetti C, Vidigal JA, Han YC, Ogrodowski P, Crippa A, Rekhtman N, de Stanchina E, Lowe SW, Ventura A. In vivo engineering of oncogenic chromosomal rearrangements with the CRISPR/Cas9 system. *Nature*. 2014;516(7531):423-427. PMID: 25337876. DOI: 10.1038/nature13902
17. Sanchez-Rivera FJ, Papagiannakopoulos T, Romero R, Tammela T, Bauer MR, Bhutkar A, Joshi NS, Subbaraj L, Bronson RT, Xue W, Jacks T. Rapid modelling of cooperating genetic events in cancer through somatic genome editing. *Nature*. 2014;516(7531):428-431. PMID: 25337879. DOI: 10.1038/nature13906
18. Singh M, Murriel CL, Johnson L. Genetically engineered mouse models: closing the gap between preclinical data and trial outcomes. *Cancer Res*. 2012;72(11):2695-2700. PMID: 22593194. DOI: 10.1158/0008-5472.CAN-11-2786
19. Zitvogel L, Pitt JM, Daillere R, Smyth MJ, Kroemer G. Mouse models in oncoimmunology. *Nat Rev Cancer*. 2016;16(12):759-773. PMID: 27687979. DOI: 10.1038/nrc.2016.91
20. Kola I, Landis J. Can the pharmaceutical industry reduce attrition rates? *Nat Rev Drug Discov*. 2004;3(8):711-715. PMID: 15286737. DOI: 10.1038/nrd1470
21. Reichert JM, Wenger JB. Development trends for new cancer therapeutics and vaccines. *Drug Discov Today*. 2008;13(1-2):30-37. PMID: 18190861. DOI: 10.1016/j.drudis.2007.09.003
22. Swindle MM, Makin A, Herron AJ, Clubb FJ, Jr., Frazier KS. Swine as models in biomedical research and toxicology testing. *Vet Pathol*. 2012;49(2):344-356. PMID: 21441112. DOI: 10.1177/0300985811402846
23. Swindle MM, Smith AC. *Swine in the Laboratory: Surgery, Anesthesia, Imaging, and Experimental Techniques*. 3rd. Boca Raton, FL: CRC Press; 2016.
24. Kuzmuk KN, Schook LB. Pigs as a Model for Biomedical Sciences. In: Rothschild MF, Ruvinsky A, editors. *The Genetics of the Pig*. Oxfordshire, UK: CABI, 2011, pp. 426-444. ISBN: 1845937562.
25. Schook LB, Collares TV, Darfour-Oduro KA, De AK, Rund LA, Schachtschneider KM, Seixas FK. Unraveling the swine genome: implications for human health. *Annu Rev Anim Biosci*. 2015;3:219-244. PMID: 25689318. DOI: 10.1146/annurev-animal-022114-110815
26. Bailey KL, Carlson MA. Porcine Models of Pancreatic Cancer. *Front Oncol*. 2019;9:144. PMID: 30915276. DOI: 10.3389/fonc.2019.00144
27. Luo Y, Li J, Liu Y, Lin L, Du Y, Li S, Yang H, Vajta G, Callesen H, Bolund L, Sorensen CB. High efficiency of BRCA1 knockout using rAAV-mediated gene targeting: developing a pig model for breast cancer. *Transgenic Res*. 2011;20(5):975-988. PMID: 21181439. DOI: 10.1007/s11248-010-9472-8
28. Schachtschneider KM, Schwind RM, Newson J, Kinachtchouk N, Rizko M, Mendoza-Elias N, Grippo P, Principe DR, Park A, Overgaard NH, Jungersen G, Garcia KD, Maker AV, Rund LA, Ozer H, Gaba RC, Schook LB. The Oncopig Cancer Model: An Innovative Large Animal Translational Oncology Platform. *Front Oncol*. 2017;7:190. PMID: 28879168. DOI: 10.3389/fonc.2017.00190

29. Flisikowska T, Kind A, Schnieke A. The new pig on the block: modelling cancer in pigs. *Transgenic Res*. 2013;22(4):673-680. PMID: 23748932. DOI: 10.1007/s11248-013-9720-9
30. Flisikowska T, Kind A, Schnieke A. Pigs as models of human cancers. *Theriogenology*. 2016;86(1):433-437. PMID: 27156684. DOI: 10.1016/j.theriogenology.2016.04.058
31. Schook LB, Collares TV, Hu W, Liang Y, Rodrigues FM, Rund LA, Schachtschneider KM, Seixas FK, Singh K, Wells KD, Walters EM, Prather RS, Counter CM. A Genetic Porcine Model of Cancer. *PLoS One*. 2015;10(7):e0128864. PMID: 26132737. DOI: 10.1371/journal.pone.0128864
32. Hingorani SR, Wang L, Multani AS, Combs C, Deramaudt TB, Hruban RH, Rustgi AK, Chang S, Tuveson DA. Trp53R172H and KrasG12D cooperate to promote chromosomal instability and widely metastatic pancreatic ductal adenocarcinoma in mice. *Cancer Cell*. 2005;7(5):469-483. PMID: 15894267. DOI: 10.1016/j.ccr.2005.04.023
33. Remmers N, Cox JL, Grunkemeyer JA, Aravind S, Arkfeld CK, Hollingsworth MA, Carlson MA. Generation of tumorigenic porcine pancreatic ductal epithelial cells: toward a large animal model of pancreatic cancer. *bioRxiv*. 2018; published online 16 February 2018; revised submission 17 May 2018. PMID: DOI: 10.1101/267112
34. Kilkenny C, Browne WJ, Cuthill IC, Emerson M, Altman DG. Improving bioscience research reporting: the ARRIVE guidelines for reporting animal research. *PLoS Biol*. 2010;8(6):e1000412. PMID: 20613859. DOI: 10.1371/journal.pbio.1000412
35. National Institutes of Health. Principles and Guidelines for Reporting Preclinical Research. Accessed 5 February 2020. Available from: https://www.nih.gov/research-training/rigor-reproducibility/principles-guidelines-reporting-preclinical-research.
36. Committee for the Update of the Guide for the Care and Use of Laboratory Animals. *Guide for the Care and Use of Laboratory Animals.* Washington, DC: The National Academies Press; 2011.
37. American Veterinary Medical Association Panel on Euthanasia. *AVMA Guidelines for the Euthanasia of Animals: 2020 Edition*. Version 2020.0.1. Schaumberg, IL: American Veterinary Medical Association; 2020. https://www.avma.org/
38. Ferrer J, Scott WE, 3rd, Weegman BP, Suszynski TM, Sutherland DE, Hering BJ, Papas KK. Pig pancreas anatomy: implications for pancreas procurement, preservation, and islet isolation. *Transplantation*. 2008;86(11):1503-1510. PMID: 19077881. DOI: 10.1097/TP.0b013e31818bfda1
39. Skandalakis LJ, Rowe JS, Jr., Gray SW, Skandalakis JE. Surgical embryology and anatomy of the pancreas. *Surg Clin North Am*. 1993;73(4):661-697. PMID: 8378816. DOI: 10.1016/s0039-6109(16)46080-9
40. Principe DR, Overgaard NH, Park AJ, Diaz AM, Torres C, McKinney R, Dorman MJ, Castellanos K, Schwind R, Dawson DW, Rana A, Maker A, Munshi HG, Rund LA, Grippo PJ, Schook LB. KRAS(G12D) and TP53(R167H) Cooperate to Induce Pancreatic Ductal Adenocarcinoma in Sus scrofa Pigs. *Sci Rep*. 2018;8(1):12548. PMID: 30135483. DOI: 10.1038/s41598-018-30916-6
41. Lutschg V, Boucke K, Hemmi S, Greber UF. Chemotactic antiviral cytokines promote infectious apical entry of human adenovirus into polarized epithelial cells. *Nat Commun*. 2011;2:391. PMID: 21750545. DOI: 10.1038/ncomms1391
42. Kotha PL, Sharma P, Kolawole AO, Yan R, Alghamri MS, Brockman TL, Gomez-Cambronero J, Excoffon KJ. Adenovirus entry from the apical surface of polarized epithelia is

facilitated by the host innate immune response. *PLoS Pathog*. 2015;11(3):e1004696. PMID: 25768646. DOI: 10.1371/journal.ppat.1004696
43. Wagner M, Koyasu S. Cancer Immunoediting by Innate Lymphoid Cells. *Trends Immunol*. 2019;40(5):415-430. PMID: 30992189. DOI: 10.1016/j.it.2019.03.004
44. Schumacher TN, Schreiber RD. Neoantigens in cancer immunotherapy. *Science*. 2015;348(6230):69-74. PMID: 25838375. DOI: 10.1126/science.aaa4971
45. Vesely MD, Kershaw MH, Schreiber RD, Smyth MJ. Natural innate and adaptive immunity to cancer. *Annu Rev Immunol*. 2011;29:235-271. PMID: 21219185. DOI: 10.1146/annurev-immunol-031210-101324
46. Tentler JJ, Tan AC, Weekes CD, Jimeno A, Leong S, Pitts TM, Arcaroli JJ, Messersmith WA, Eckhardt SG. Patient-derived tumour xenografts as models for oncology drug development. *Nat Rev Clin Oncol*. 2012;9(6):338-350. PMID: 22508028. DOI: 10.1038/nrclinonc.2012.61

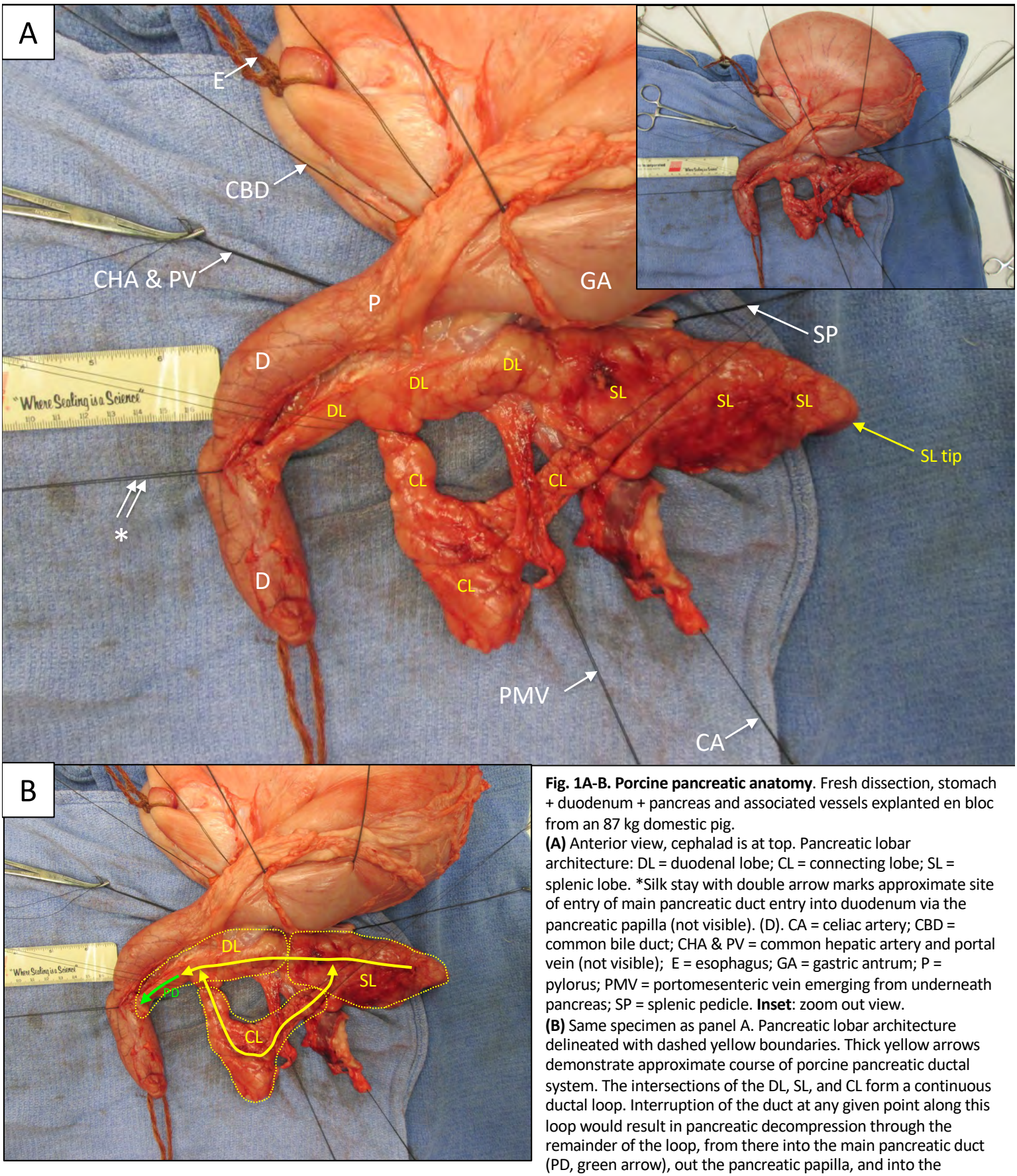

Fig. 1A-B. Porcine pancreatic anatomy. Fresh dissection, stomach + duodenum + pancreas and associated vessels explanted en bloc from an 87 kg domestic pig.
(A) Anterior view, cephalad is at top. Pancreatic lobar architecture: DL = duodenal lobe; CL = connecting lobe; SL = splenic lobe. *Silk stay with double arrow marks approximate site of entry of main pancreatic duct entry into duodenum via the pancreatic papilla (not visible). (D). CA = celiac artery; CBD = common bile duct; CHA & PV = common hepatic artery and portal vein (not visible); E = esophagus; GA = gastric antrum; P = pylorus; PMV = portomesenteric vein emerging from underneath pancreas; SP = splenic pedicle. **Inset**: zoom out view.
(B) Same specimen as panel A. Pancreatic lobar architecture delineated with dashed yellow boundaries. Thick yellow arrows demonstrate approximate course of porcine pancreatic ductal system. The intersections of the DL, SL, and CL form a continuous ductal loop. Interruption of the duct at any given point along this loop would result in pancreatic decompression through the remainder of the loop, from there into the main pancreatic duct (PD, green arrow), out the pancreatic papilla, and into the duodenum.

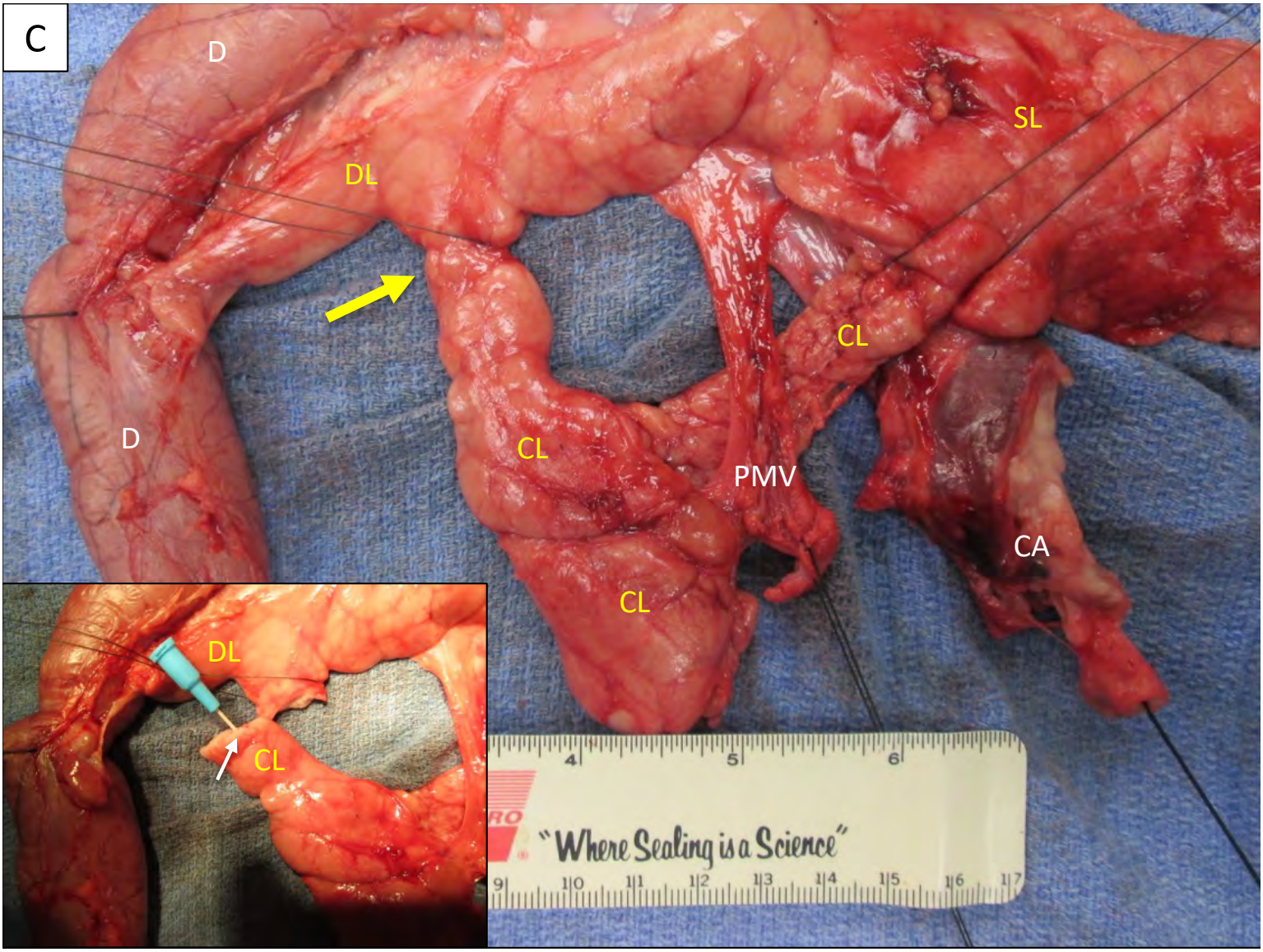

Fig. 1C. Porcine pancreatic anatomy. Continued. **(C)** Zoom in view of same specimen shown in Fig. 1. Yellow arrow indicates location of CL transection for injection into the CL duct. **Inset**: CL has been disconnected from DL; a 22g plastic catheter has been inserted (small white arrow) into the main duct of the CL (mimic of *in vivo* CL injection procedure).

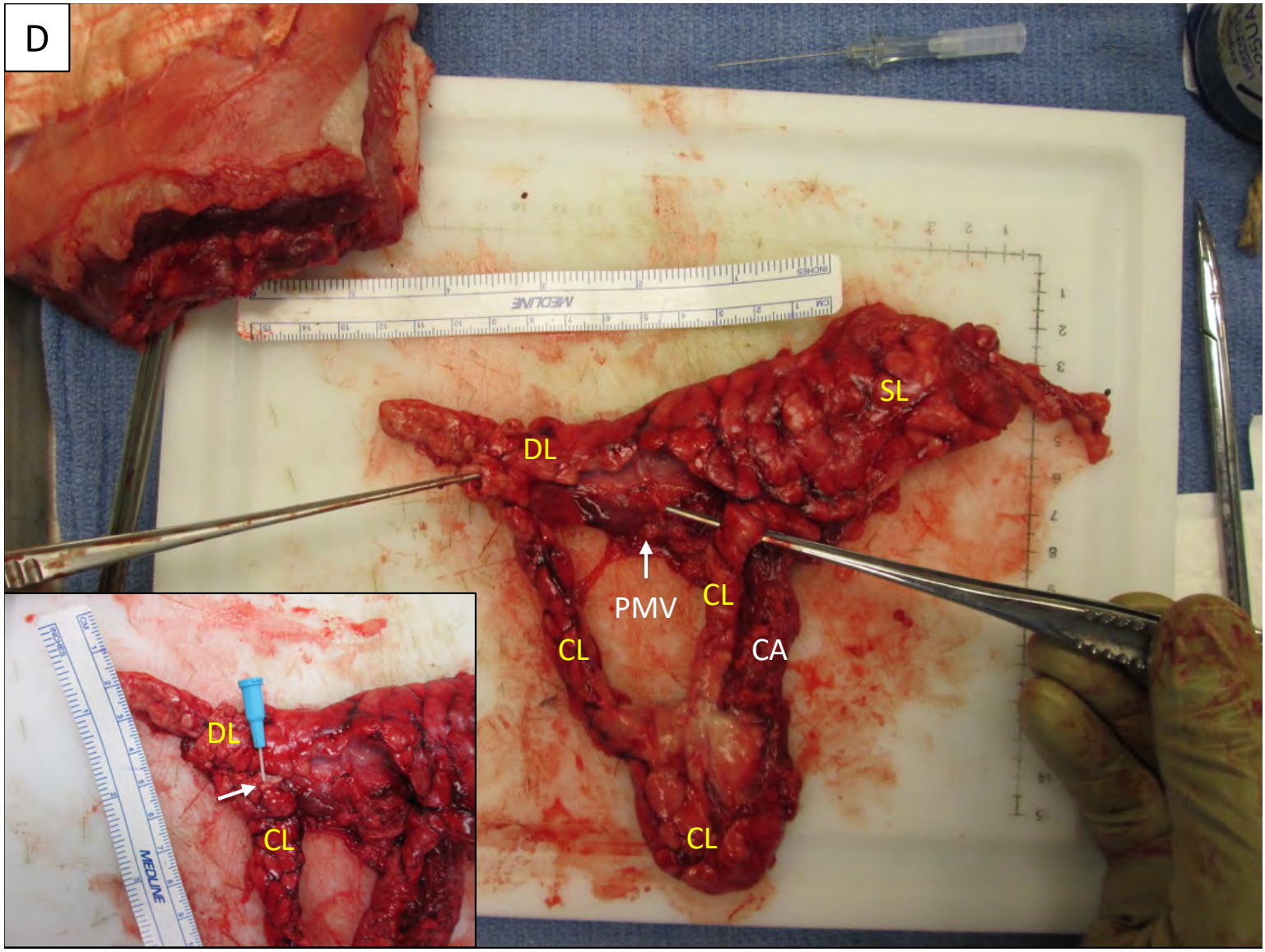

Fig. 1D. Porcine pancreatic anatomy. Continued. **(D)** Fresh dissection, stomach + duodenum + pancreas and associated vessels explanted en bloc from a second domestic pig (85 kg at euthanasia). This subject is shown simply for corroboration of panels A-C. The difference between this subject and that in panels A-C is that this subject had harvest of the proximal DL and distal tip of the SL for PDEC culture, and that the duodenum and stomach were not taken en bloc. But this dissection also demonstrates the full-circle anatomy of the CL, which is connected proximally to the DL and distally to the SL. **Inset**: cannulization of the CL duct with a 22g plastic catheter; the CL has been transected near its terminus into the DL, similar to that shown in panel C.

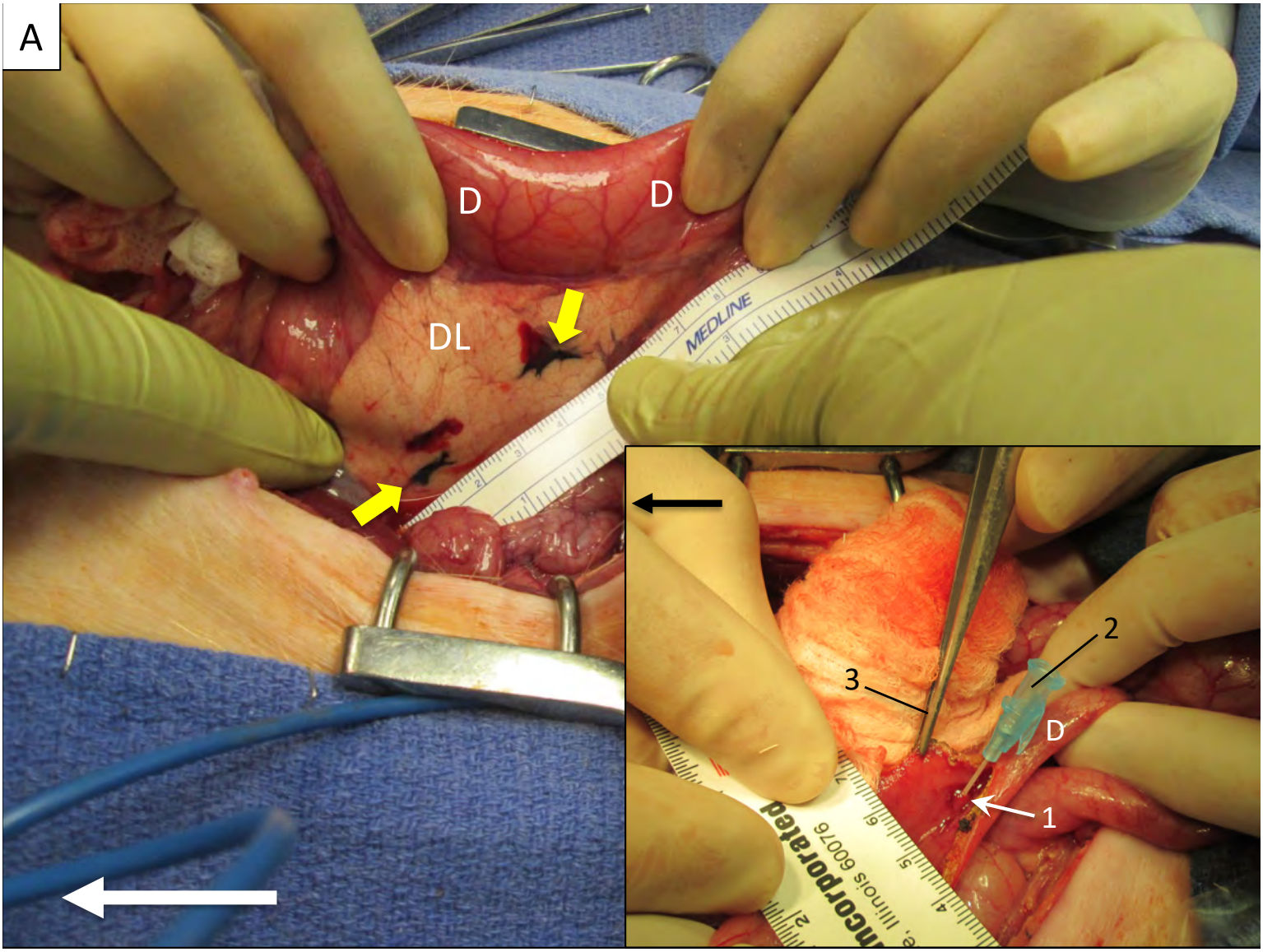

Fig. 2A. Subject 468. This was the first subject in the series; it expired unexpectantly 18 days after tumor induction.
(A) Tumor induction procedure. The pancreas was exposed through an upper midline incision. The posterior surface of the duodenal lobe (DL) of the pancreas (shown) was marked at two sites with India Ink (yellow arrows). AdCre (10^{10} viral particles in 100 µL saline) was injected into the pancreatic parenchyma at each site using a 27g needle. The anterior surface was then exposed, and similar injections were performed into the parenchyma on the anterior pancreas. Next, the duodenal insertion of the main pancreatic duct was identified at the terminus of the duodenal lobe on the mesenteric border of the duodenum. A longitudinal duodenotomy was made on the anti-mesenteric side of the duodenum, just opposite to the insertion of the main pancreatic duct (**Inset**). The pancreatic papilla (1) was identified within the duodenal lumen and cannulated with a 20g Angiocath (2). Debakey forceps (3) is shown retracting duodenal wall at site of duodenotomy. AdCre solution (100 µL) was then injected directly into the main pancreatic duct via the papilla. The Angio cath was withdrawn, and the duodenotomy was then closed in two layers. D = duodenum; large white arrow & small black arrow (inset) = cephalad.

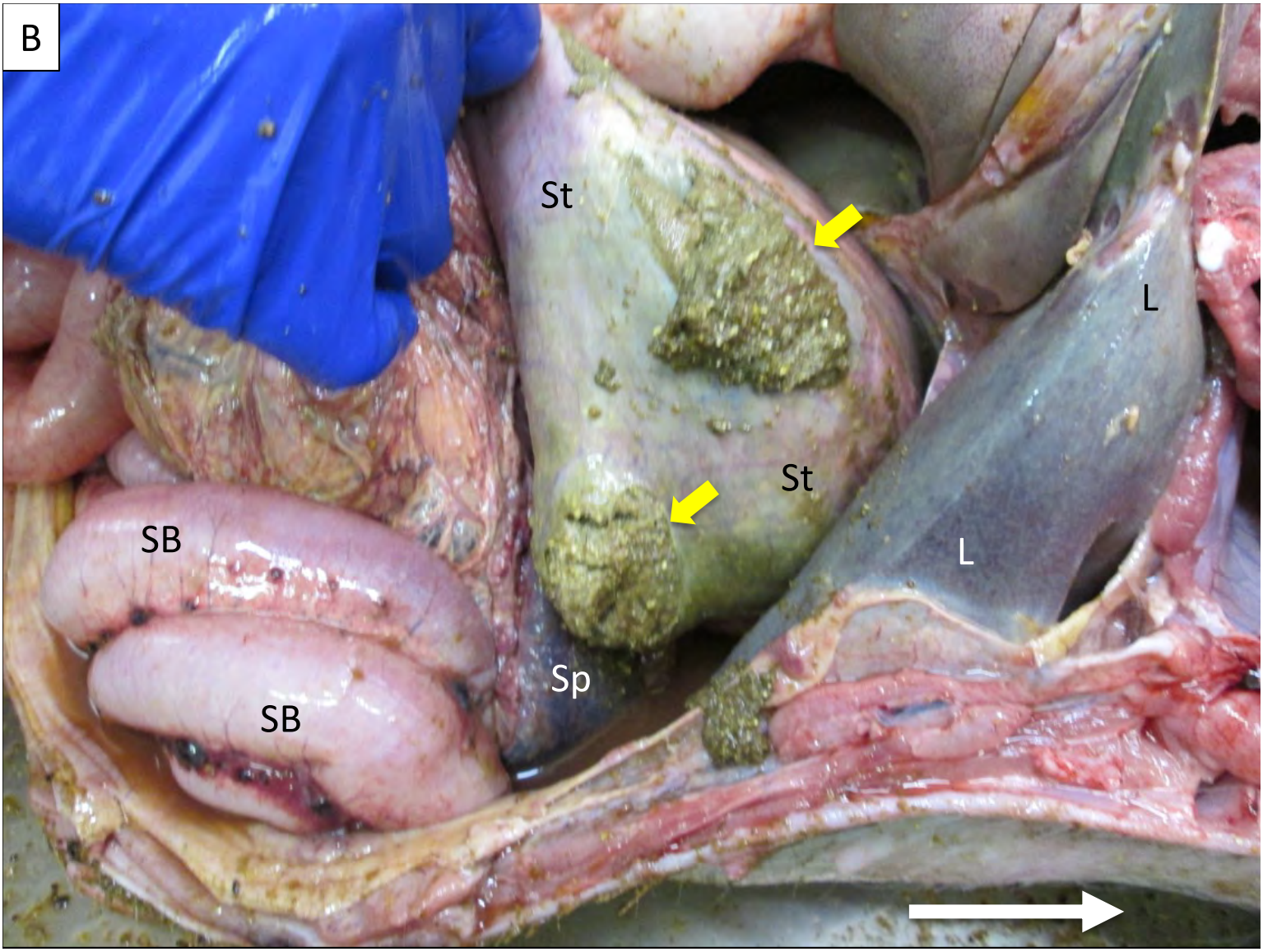

Fig. 2B. Continued. **(B)** Pig expired in evening of postoperative day 18, after 1 wk of lethargy & poor po intake. Upon re-entering the abdomen at necropsy, ~1L of clear-brown ascites was encountered. Two adjacent perforations were found in the fundus of the stomach (yellow arrows), and copious amounts of gastric contents had spilled into the peritoneal cavity. The stomach was still distended with feed, however. The stomach and pylorus were opened with a longitudinal incision. The pylorus was patent and the segment of duodenum where the anastomosis was located was identified. The suture line of the anastomosis was intact, patent, and without inflammation or reaction. Distal to that was a hemorrhagic segment of bowel with a mass effect (**C**, next page), adjacent to the site of location of the pancreatic injection. This section of bowel was not patent (i.e., it was the site of the obstruction which produced the gastric distention which led to the perforations. The rest of the pancreatic parenchyma felt firm and was hemorrhagic. The subject had lab testing 24 h prior to expiration: WBC = 17K; Hb = 13.7; plt = 255K; glucose = 134; bicarbonate = 40; creatinine = 2.0; amylase = 563; AST = 41; Tbili = 0.2.

Key: L = liver; SB = small bowel; Sp = spleen; St = stomach; small yellow arrows = perforations in the gastric fundus; large white arrow = cephalad.

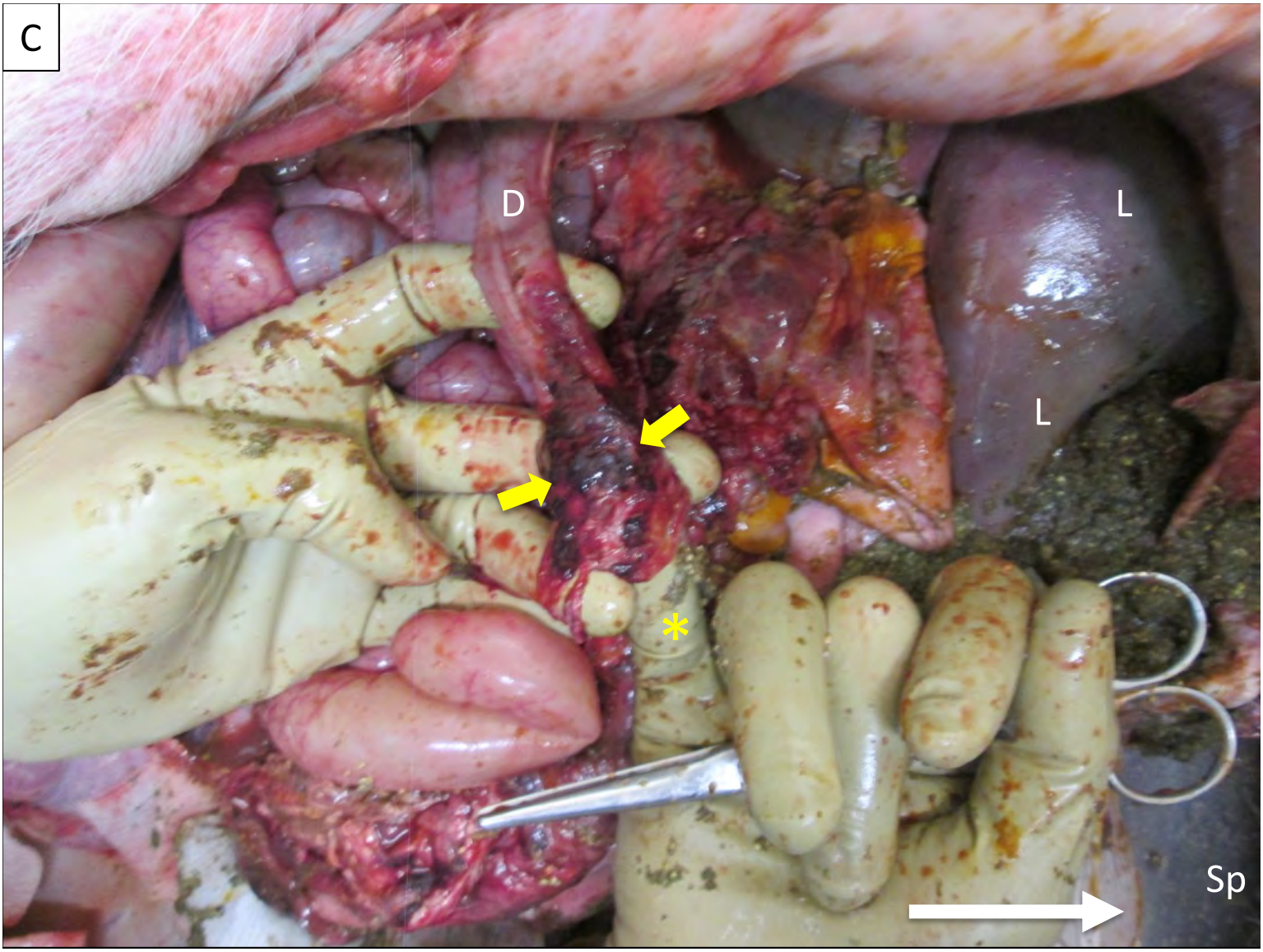

Fig. 2C. Continued. **(C)** Site of duodenal obstruction with mass effect. Finger (*) is shown inserted into proximal duodenum, but it is unable to traverse the distal duodenum at location of obstruction (yellow arrows). D = duodenum (distal, decompressed); large white arrow = cephalad.

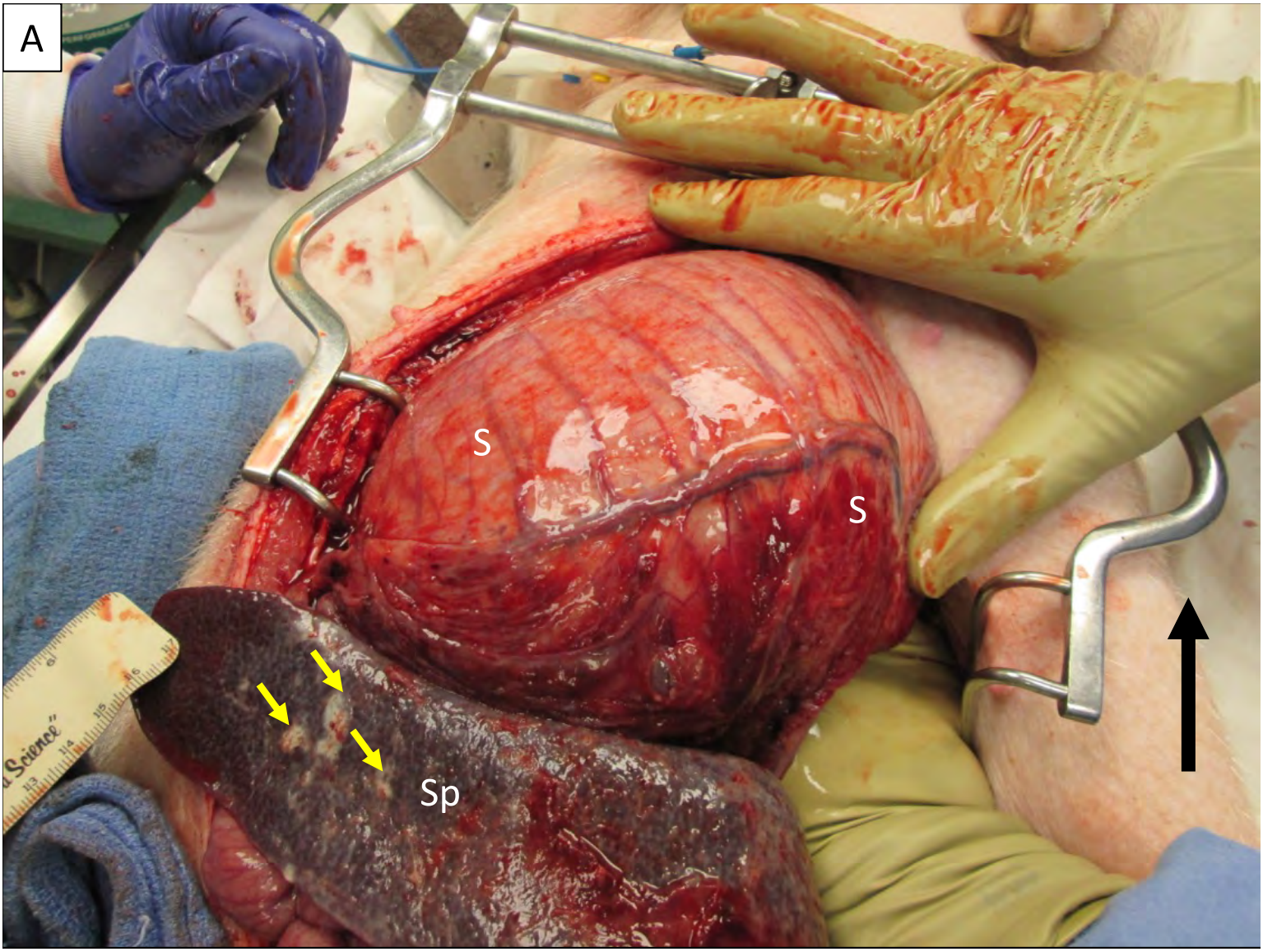

Fig. 3A. Subject 472. This subject was euthanized 14 days after the tumor induction procedure because of inability to eat. At the induction procedure, the pancreas was exposed through an upper midline incision. An injection into the duct of the connecting lobe then was performed. **(A) Necropsy.** The stomach (S) was distended with feed. The spleen (Sp) had multiple whitish plaques (yellow arrows). Similar to previous subjects, the primary cause of death in this Oncopig appeared to be hemorrhagic pancreatitis which produced extensive intraabdominal inflammation, with functional gastric outlet obstruction (ileus) and failure to thrive.

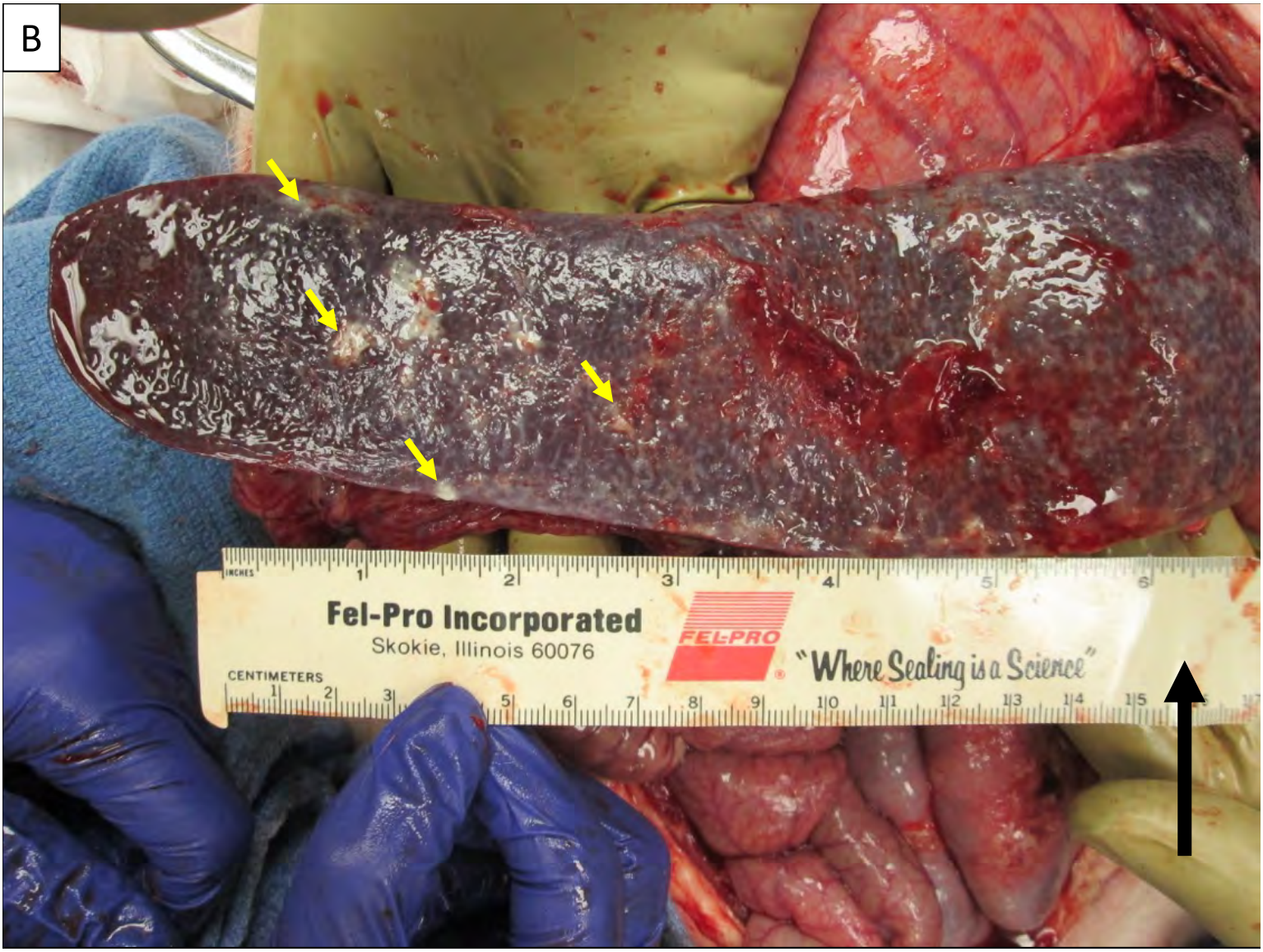

Fig. 3B. Continued. **(B) Necropsy**. Close-up view of the spleen, demonstrating multiple flat, whitish plaques (yellow arrows), 1-5 mm in diameter. Large black arrow = cephalad.

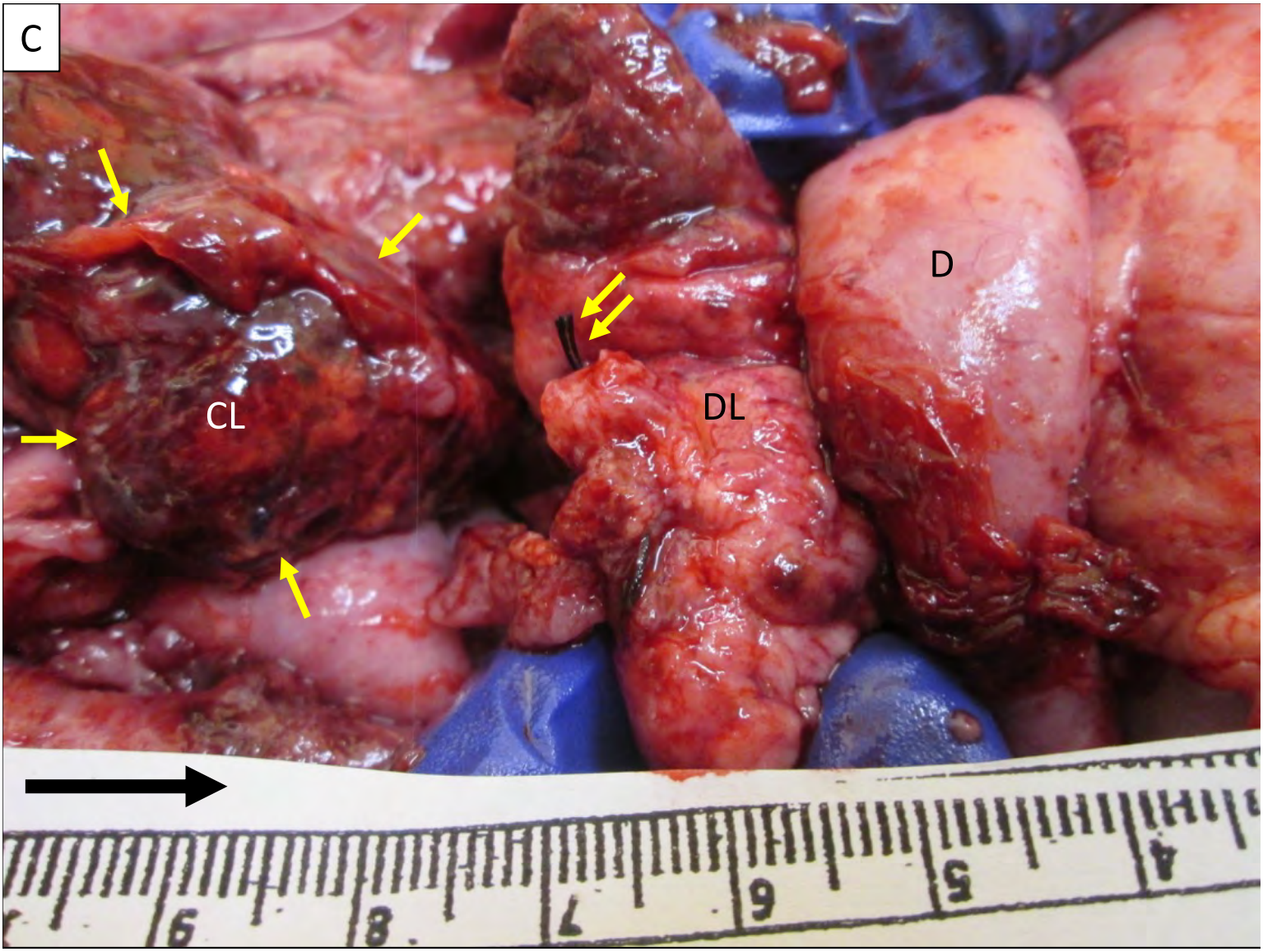

Fig. 3C. Continued. **(C) Necropsy**. The phlegmon in panel C was bluntly dissected with fingers. The duodenal lobe (DL) was identified, with a silk suture (double yellow arrow) marking the site where the proximal side of the connecting lobe (CL) had been ligated. The remnant of the CL (marked with single yellow arrows) was adjacent to this suture. D = duodenum; large black arrow = cephalad.

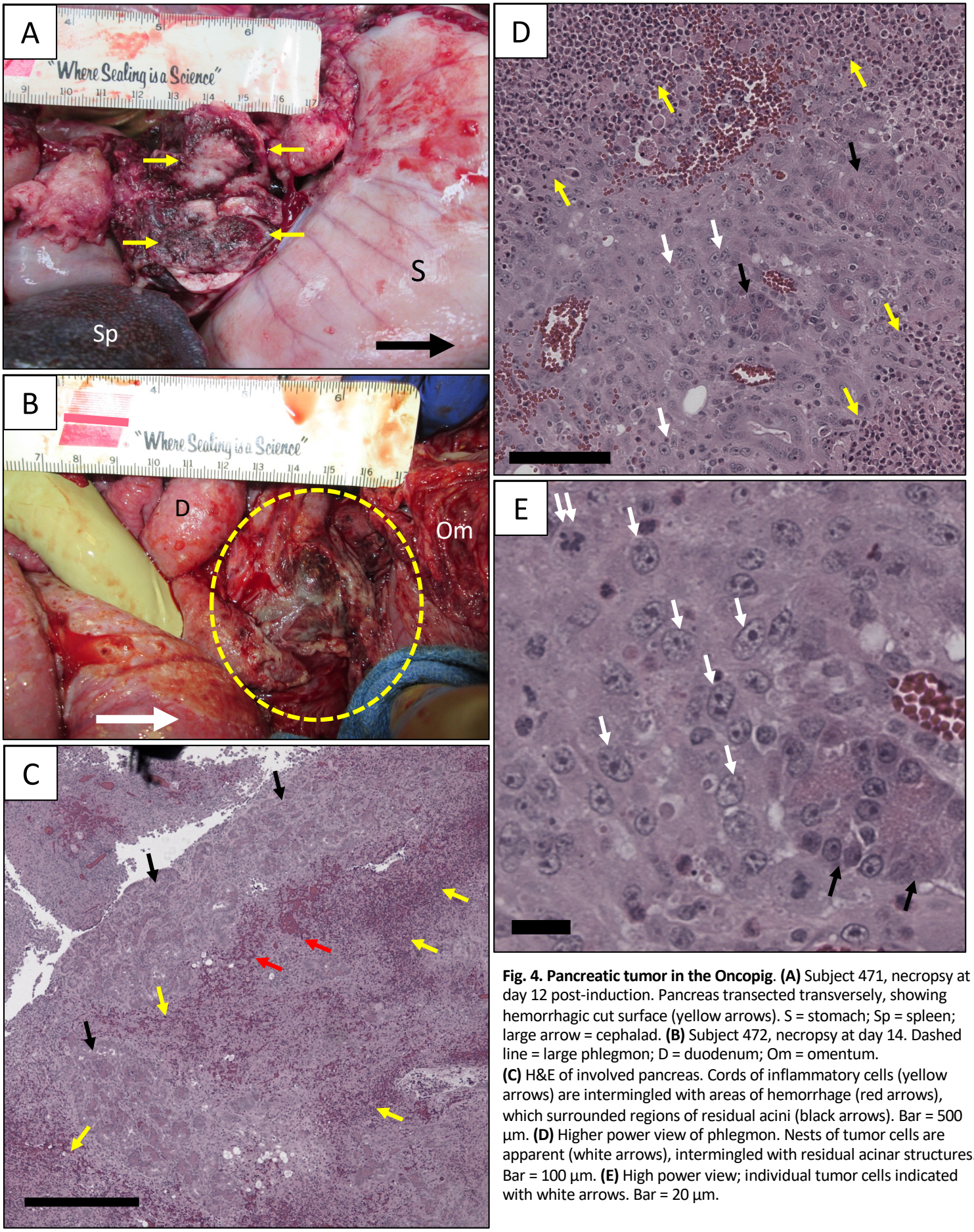

Fig. 4. Pancreatic tumor in the Oncopig. **(A)** Subject 471, necropsy at day 12 post-induction. Pancreas transected transversely, showing hemorrhagic cut surface (yellow arrows). S = stomach; Sp = spleen; large arrow = cephalad. **(B)** Subject 472, necropsy at day 14. Dashed line = large phlegmon; D = duodenum; Om = omentum. **(C)** H&E of involved pancreas. Cords of inflammatory cells (yellow arrows) are intermingled with areas of hemorrhage (red arrows), which surrounded regions of residual acini (black arrows). Bar = 500 µm. **(D)** Higher power view of phlegmon. Nests of tumor cells are apparent (white arrows), intermingled with residual acinar structures. Bar = 100 µm. **(E)** High power view; individual tumor cells indicated with white arrows. Bar = 20 µm.